Histol Histopathol (1999) 14: 687-695

http://www.ehu.es/histol-histopathol

Histology and Histopathology

Double-sided staining with a gold probe and silver enhancement to detect α-amylase and sugar moieties in the mouse salivary glands

G. Menghi, L. Marchetti, A.M. Bondi, D. Accili, M.G. Sabbieti and G. Materazzi

Department of Comparative Morphological and Biochemical Sciences, University of Camerino, Camerino, Italy

Summary. In the present study we report the development of an ultrastructural electron microscopic double-sided staining technique that, using gold probes of 10 nm and enhancement of the gold signal by silver amplification, allows the demonstration of two antigenic sites on the same section. The labeling was carried out in the following manner: one face of uncoated floating grids was incubated with an antibody directed to α-amylase, followed by a secondary gold-labeled antibody, amplification of gold particles, drying and carbon coating; subsequently, the reverse face of the same grid, was processed for lectin cytochemistry, with and without sialidase digestion, and it was incubated with HRP-conjugated lectins, anti-HRP antibody and protein-A gold. Also the reverse sequence of steps and amplification of gold signal after the first or second labeling were experimented. The resultant small and large particles revealed different distributional patterns of antigenic sites on the opposite faces of the same tissue section. The transparency of the resin-embedded ultrathin sections in the electron beam allowed the simultaneous visualization of the gold probes of different sizes present on the two faces. The analysis of immunolabeling revealed that the α-amylase is chiefly secreted by the parotid and submandibular glands. The application of this double-sided staining technique also indicated that, when present in glycosylated form, the α-amylase enzyme does not contain sialic acid in the submandibular and sublingual glands; conversely, its location on the electron-dense areas of target granules in the parotid acinar cells seems to suggest that a sialylated isoenzymatic form can occur within these granule regions where sialic, acid linked to ß-galactose, was found to be located.

Key words: α-amylase, carbohydrates, lectins, immunogold, silver enhancement, salivary glands, mouse

Offprint requests to: Prof. Giovanna Menghi, Dipartimento di Scienze Morfologiche e Biochimiche Comparate, Università di Camerino, Via Gentile III da Varano, I-62032, Camerino (MC), Italy. Fax: (737) 402708

Introduction

Amylase is a widely distributed enzyme in nature where it is produced by bacteria, fungi, plants and animals. In addition, amylases display a relatively high level of evolutionary conservation documented by common characteristics, namely molecular weight, ranging between 55 and 60 kD, secondary structure of the catalytic site and dependence on calcium ions (Mackay et al., 1985; Nakajima et al., 1986; MacGregor, 1988). Amylases have attracted considerable attention, especially in the bacterial and fungal enzymes because of their commercial value, while mammalian amylases have been studied extensively owing to their clinical significance (Matsuura et al., 1984; Meisler and Gumicio, 1986; Buisson et al., 1987). In mammals amylase occurs in two different isoforms, i.e. salivary and pancreatic amylase that are rather similar; in the mouse it has been demonstrated that the two proteins only differ for 12 per cent of the aminoacid sequence and the specificity seems to be slightly different (Hagenbuche et al., 1980). In human beings, further differences have been found between the two main types; indeed, in the salivary amylase, Keller et al. (1971) discriminated between two enzyme families: the former composed of non-glycosylated isoenzymes, the latter composed of three glycosylated isoforms containing N-acetylglucosamine, glucose, mannose, and galactose. N-glycosidic linkage between the carbohydrate and protein portion has also been demonstrated (Tollefsen and Rosenblum, 1988). The aminoacid sequence found in the human amylase resulted to be about 80 per cent similar to that of mouse corresponding enzyme (Tokunaga et al., 1987, 1988, 1991, 1992). Also in the mouse, glycosylated and non-glycosylated α-amylase isoforms have been found and the occurrence of mannose and N-glycosidic linkage has been ascertained (Tokunaga et al., 1991).

The present research is aimed to study the occurrence of α-amylase in the mouse major salivary glands and the subcellular codistribution, and/or differential distribution of the α-amylase molecule and

sugar residues in order to apport further elements to the definition of glycosylation type of salivary amylase. To this purpose, double-sided immunogold techniques making use of a gold probe of 10 nm on both sides of the grid and silver enhancement of gold signal on one side only were experimented at electron microscope level.

Materials and methods

Animals

Parotid, submandibular and sublingual glands from sexually mature white mice *(Mus musculus)*, Swiss strain (Stock Morini, S. Polo d'Enza, RE, Italy), of both sexes (6 males and 6 females), were used. The animals, fed *ad libitum*, were kept at 12d:12l regimen and sacrificed by CO_2 suffocation according to the recommendations of the Italian Ethical Committee and under the supervision of authorized investigators.

Tissue preparation

Immediately after removal, tissues were fixed according to previously detailed protocols and dehydrated with increasing acetone concentrations up to 90% (Menghi et al., 1996a,b). Samples were then embedded in Unicryl (British BioCell Int. Ltd) according to previous researches (Menghi et al., 1998b). Ultrathin sections, about 60 nm thick, obtained with a LKB Ultrotome V were collected on 400-mesh uncoated nickel grids.

Double-sided staining method

The double staining method employed here requires the application of the two different protocols, performed in alternate sequence of labeling and silver amplification, on the two faces of the grids, as follows:

a) α-amylase immunostaining on one face of the grid

Short-time collected ultrathin sections, rehydrated with distilled water and 0.05M TBS (Tris Buffered Saline), pH 7.6, were kept 20 min on a drop of 1% BSA (Bovine Serum Albumin)-TBS, and incubated with anti-human α-amylase raised in rabbit (Sigma Chemical Co. St. Louis, MO, USA) diluted 1:100 in 0.05M TBS, pH 7.6, containing 1% BSA and 5% NGS (Normal Goat Serum) for 40 min at room temperature. After rinsing in TBS, sections were incubated in goat anti-rabbit IgG conjugated with 10 nm colloidal gold (Auroprobe GAR EM G10, Amersham Life Sciences) diluted 1:10 in 0.05M TBS, pH 7.6, containing 0.05% Tween 20 for 60 min at room temperature. Sections were then rinsed many times in TBS and distilled water prior to amplifying the gold signal with IntenSE M kit (Amersham) for 3 min at room temperature. Finally, in order to prevent non-specific labeling, this face of the grid was dried, coated with a carbon film of about 15 nm by means of a turbo mini high vacuum deposition system (MED010, Balzers Union) and turned over for the second binding process on the other face.

b) Lectin cytochemistry and enzymatic digestion on the other face of the grid

Sections were treated for the detection and visualization of terminal and subterminal sugar residues. The following lectins, conjugated with HRP (Horseradish Peroxidase), were tested: DBA (from *Dolichos biflorus*, for α-N-acetylgalactosamine), PNA (from *Arachis hypogaea*, for ß-galactose), Con A (from *Canavalia ensiformis*, for D-mannose>D-glucose), WGA (from *Triticum vulgaris*, for N-acetylglucosamine) at a concentration of 2 μg/ml, and LTA (from *Tetragonolobus purpureas*, for α-L-fucose) at a concentration of 10 μg/ml. All lectins were purchased from Sigma. After re-hydration, the appropriate face of floating grids was incubated with HRP-conjugated lectins dissolved in 0.1M TBS added with 1% BSA for 2 h, at room temperature, rinsed with 0.05M TBS containing 1% BSA and reacted with rabbit anti-HRP antibody (Sigma) diluted 1:100 in TBS-BSA for 60 min, rinsed in TBS-BSA, and then incubated with protein A-gold (10 nm, Sigma) diluted 1:50 in TBS-BSA added with 0.05% Tween 20 for 60 min. After final washing, grids were counterstained with uranyl acetate (10 min at 30 °C) and lead citrate (1 min at 20 °C) by an LKB Ultrostainer and analyzed in a Philips 201C TEM.

In order to obtain additional information about the sialic acid acceptor sugars, some grids were digested with sialidase (neuraminidase type V, from *Clostridium perfringens*, 0.5 U/ml in acetate buffer, pH 5.5, plus 10mM $CaCl_2$ for 16h at 37 °C) before lectin binding as previously detailed (Menghi et al., 1996b, 1998b).

Controls

Controls for α-amylase specificity were performed by omitting the primary antibody and by pre-incubating the antiserum in an excess of human salivary amylase (Sigma, Type IX-A).

Controls to verify the nominal affinity of lectins were carried out by adding the respective competing sugars to the lectin solutions at concentrations ranging from 0.2 to 0.4M. Also the omission of the lectin conjugates or antiperoxidase antibody was tested.

The efficacy of sialidase enzyme was tested by treating control grids with enzyme-free buffer under the above conditions and by using lectins recognizing sialic acid after digestion.

Results

The silver enhancement represents a technique allowing the size of a gold particle to be increased by silver precipitation catalyzed by gold without enhancing their number (Bendayan, 1995). Preliminary experi-

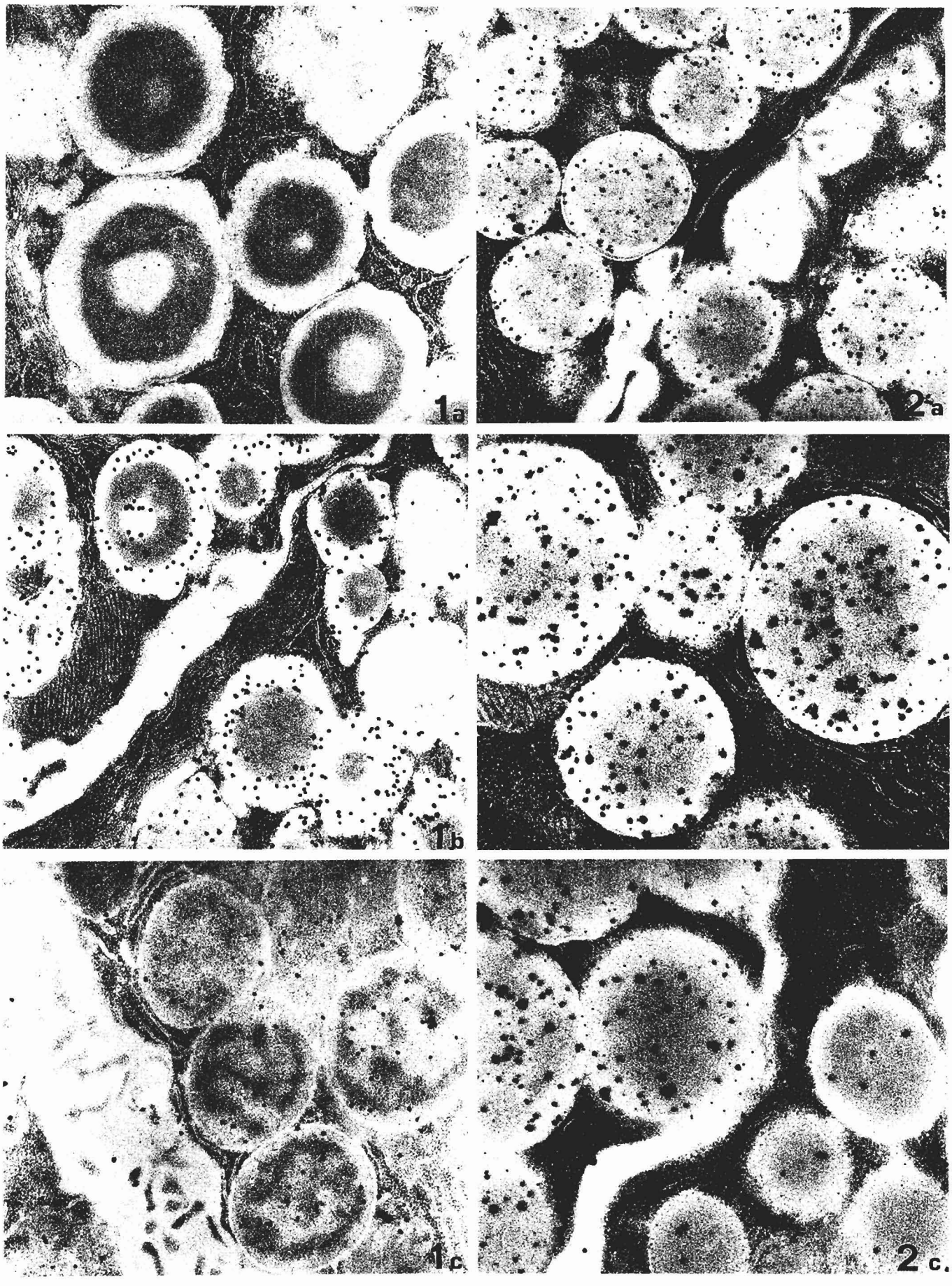
1a
2a
1b
1c
2c

Fig. 1. Parotid gland. Electron micrographs of acinar cell secretory granules labeled immunocytochemically with antibody to α-amylase. Native gold signal **(a)** and silver enhanced gold signal **(b, c)**. a, x 28,300; b and c, x 26,400

Fig. 2. Parotid gland. Double-sided staining with antibody to α-amylase on both faces and silver amplification on one face only. Non-amplified binding sites of one face (small particles) and amplified binding sites of the opposite face (large particles) confirmed that the enzyme is not preferentially located on electron-dense or electron-lucent areas of the granule matrix **(a, b)**. Conversely, the intensity of binding showed marked differences between adjacent cells regardless of the types of granules contained **(c)**. a, x 26,400; b and c, x 42,500

ments, aimed to find the optimal conditions for employing the silver enhancer for electron microscopy, revealed that the carbon coating must be carried out after silver amplification following the first step of labeling method; in addition, the optimal time of amplification at room temperature was found to be 3 min (Menghi et al., 1997).

Technical aspects were satisfactory and resulted in an acceptable morphology; both the lectin affinity patterns and specificity of α-amylase binding gave evidence of a satisfactory preservation of sugar residues and good retention of antigenic sites, respectively.

Parotid gland

The α-amylase occurrence was visualized with different intensity on the polymorphous secretory granules and exhibited distributional patterns on granule matrix without marked preference for electron-lucent or electron-dense zones of bizonal and mottled granules (Fig. 1a-c). The independent visualization of enzyme on both the sides of sections revealed that there was no codistribution of binding on the opposite faces of the samples (Fig. 2a-c).

The double-sided staining with α-amylase and lectins LTA (Fig. 3a), WGA (Fig. 3b), Con A (Fig. 3c) revealed randomly distributed binding sites of enzyme and sugars.

The double binding with α-amylase and DBA (Fig. 3d) and sialidase/DBA gave binding patterns without characteristic distribution of small and large particles. As concerns the double binding of α-amylase with PNA (Fig. 3e) and sialidase/PNA (Fig. 3f), a concentration of gold signals of both sizes was observed on darker zones of target granules.

Submandibular gland

Results did not evidence appreciable differences between sexes. In males and females α-amylase was located on the electron-dense granules of convoluted granular tubule cells and the double-sided staining with only the enzyme did not exhibit appreciable differences of intensity on the two faces of the grids although binding sites occurred in different location sites within the same secretory granules (Figs 4a, 5a). Double stained acinar cell electron-lucent granules did not exhibit α-amylase immunostaining on either face.

Also the double-sided staining with both enzyme and LTA (Fig. 4b), WGA, Con A (Fig. 4c), PNA (Fig. 5b), and DBA lectins, showed no differences between sexes on the convoluted granular tubule electron-dense granules where enzyme and sugars were visualized. Conversely, in contrast to the lack of enzyme in the acinar cell electron-lucent granules, occurrence of DBA (Fig. 5c) and heterogeneous sialoglycoconjugates was found.

Sublingual gland

The α-amylase location was restricted to the electron-dense granules of demilunar cells and showed a modest reactivity as well as marked variability of binding between adjacent secretory granules (Fig. 6a).

The double-sided staining with amylase and lectins LTA (Fig. 6b), WGA (Fig. 6c), Con A (Fig. 6d), DBA (Fig. 6e), and PNA (Fig. 6f) showed few affinity sites on demilune cell electron-dense granules; acinar cells did not present enzyme occurrence at electron-lucent secretory granule level where sialoglycoconjugates linked to ß-galactose and α-N-acetylgalactosamine were located.

Discussion

The double-sided staining method provides for the application of two different protocols performed in adequate sequence on the two faces of the same grid. The α-amylase immunolabeling and lectin cytochemistry, combined with sialidase digestion, were carried out in different order and combination to identify each type of interference between procedures performed on the two sides and to verify the validity and advantage of double-sided staining. The amplification of the gold signal, alternatively on one of the two faces of the same section, showed comparable intensity of binding; moreover, present findings evidenced that the carbon film did not appreciably affect binding performed on the opposite side of the grid and besides led samples to

Fig. 3. Parotid gland. Double-sided staining. Note the binding sites of lectins LTA **(a)**, WGA **(b)**, Con A **(c)**, DBA **(d)**, PNA **(e)**, and sialidase/PNA **(f)** with amplified gold signal (large particles) on one face of the grid and the α-amylase immunolabeling (small particles) on the other face of the same section. Some codistribution of sites occurred above all for PNA and sialidase/PNA binding patterns at electron-dense zones of target granules (e, f). a and d, x 42,500; b, c, e and f, x 39,600

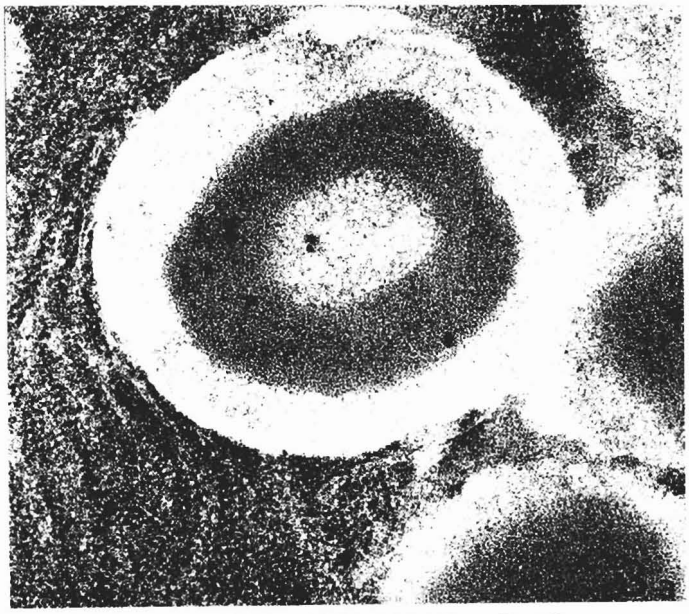

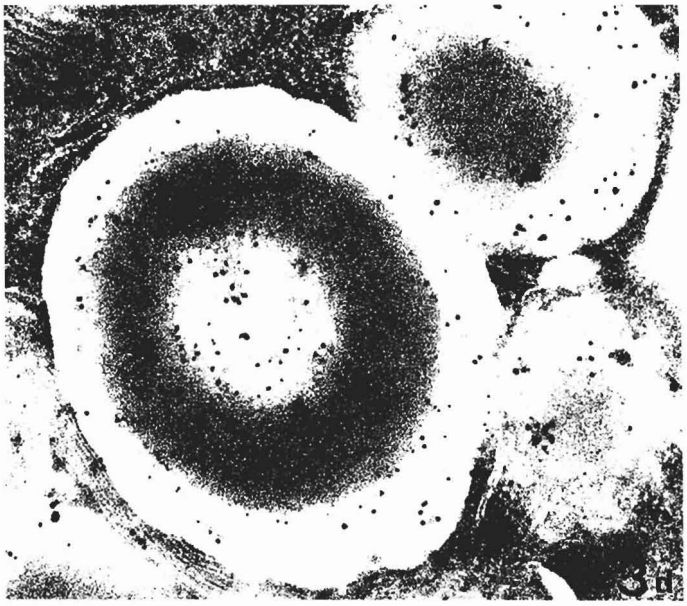

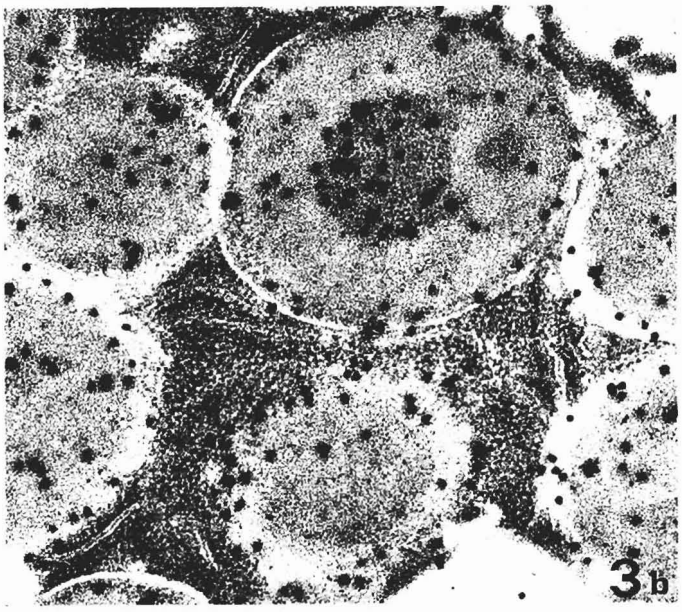
3b

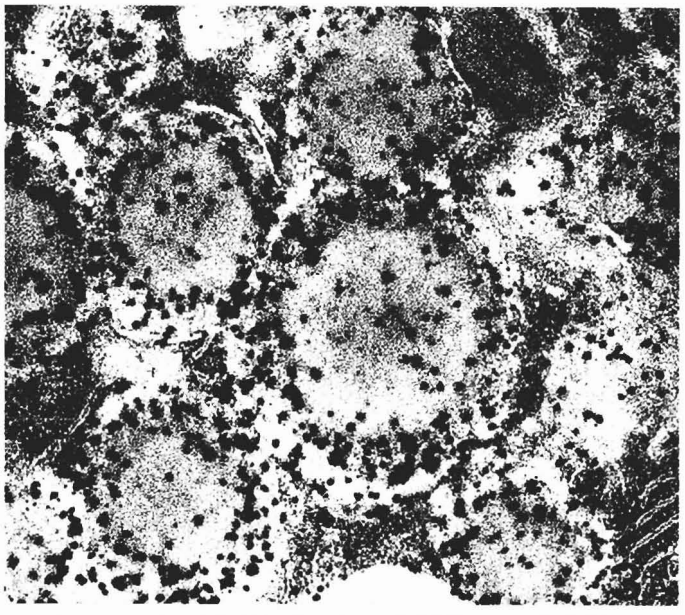

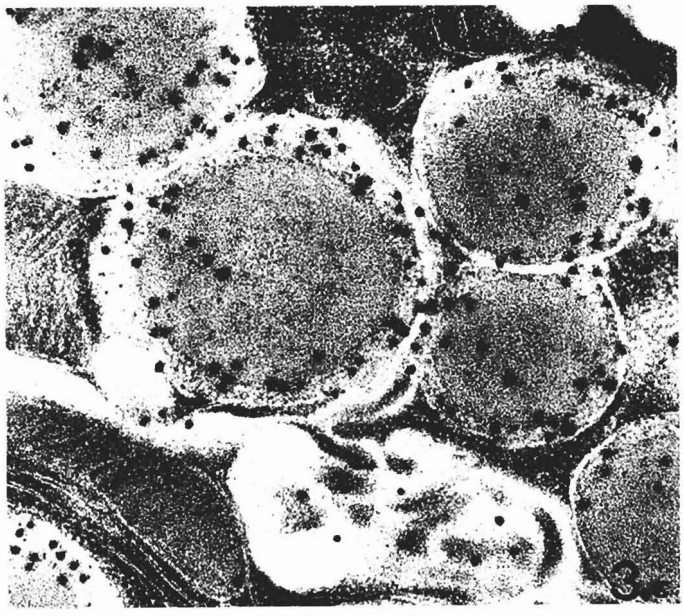
3

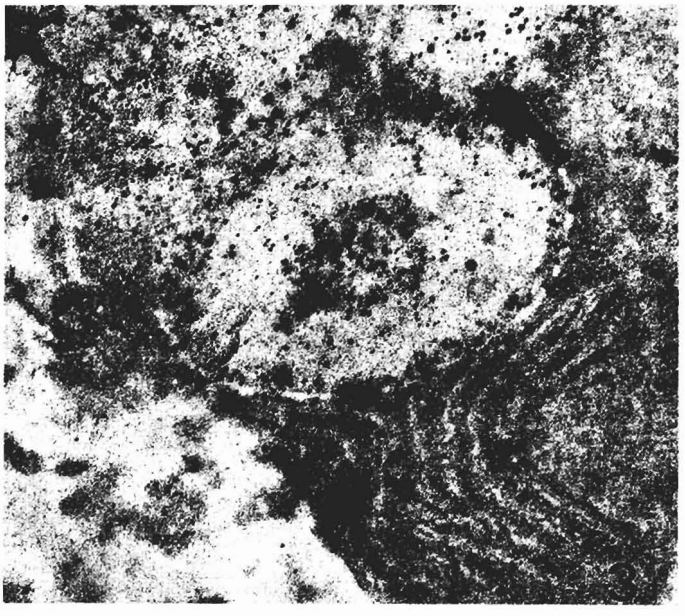

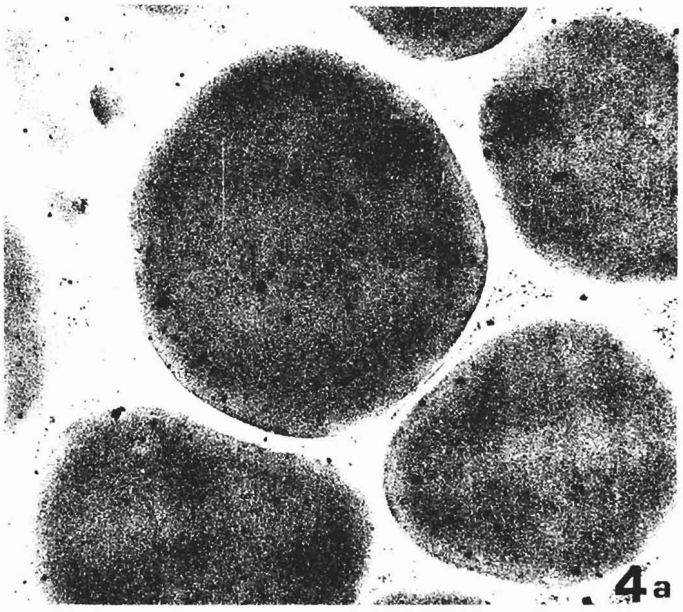

4a

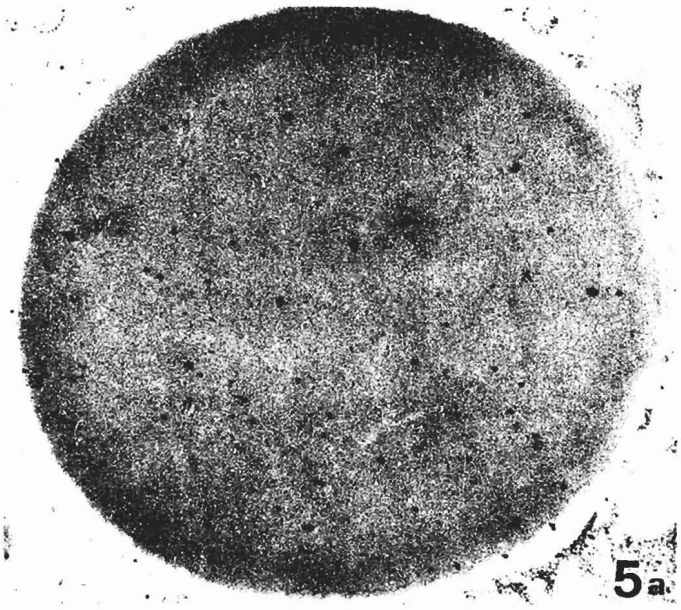

5a

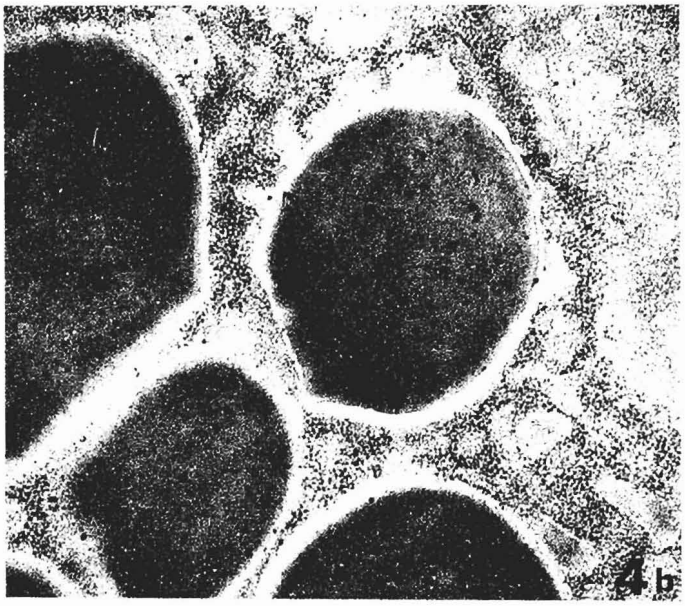

4b

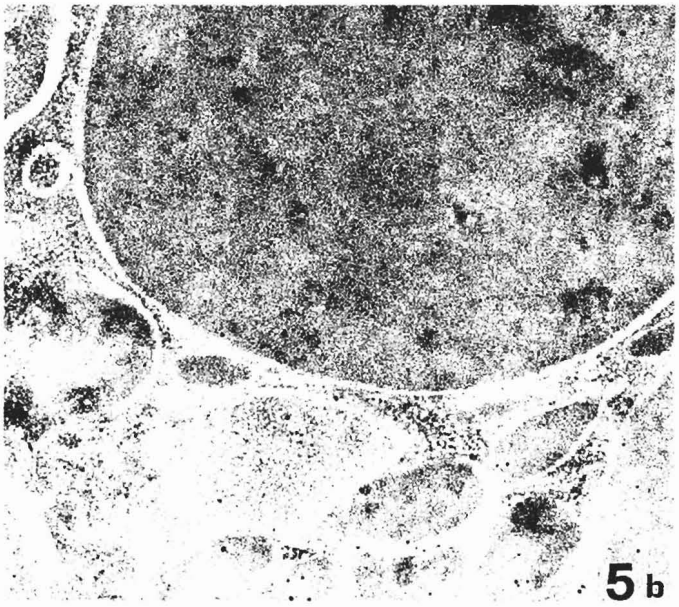

5b

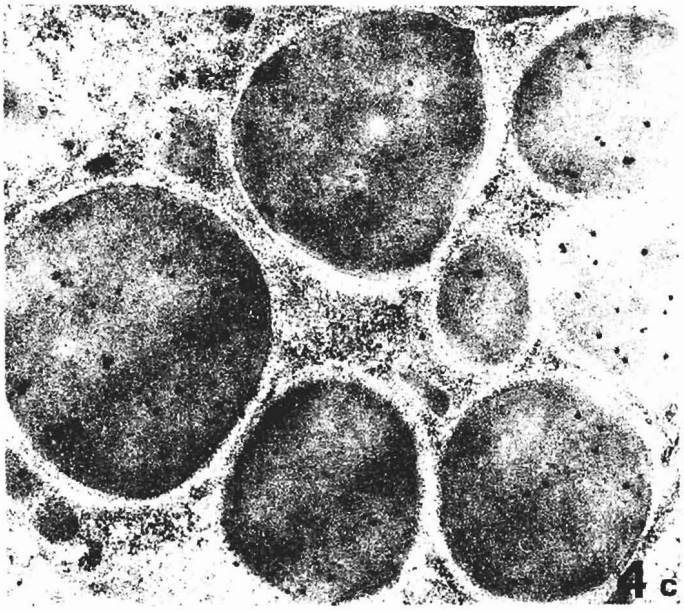

4c

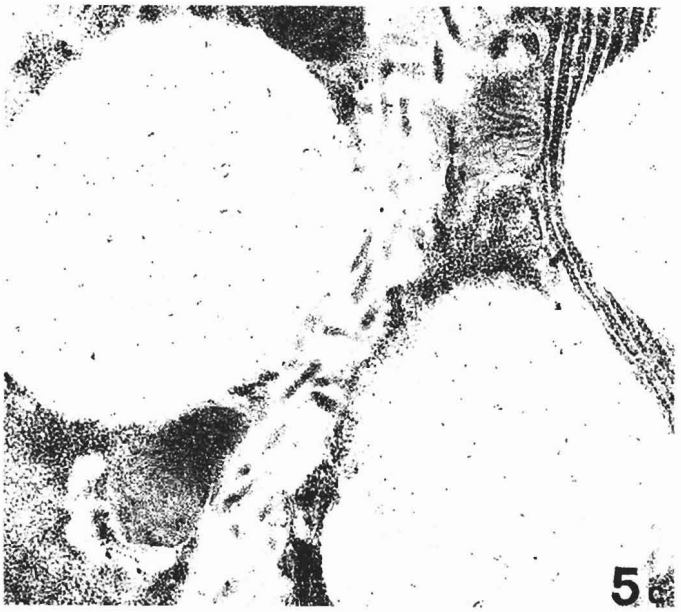

5c

Fig. 4. Female submandibular gland. Double-sided α-amylase immunostaining with native (small particles) and amplified (large particles) gold signal **(a)**; it should be noted the uncoincidence of positive sites on the two faces of the same secretory granule of convoluted granular tubules. Double-sided staining with α-amylase non-amplified gold signal (small particles) and LTA **(b)**, Con A **(c)** silver enhanced gold signal (large particles) in the convoluted granular tubule secretory granules. x 26,400

Fig. 5. Male submandibular gland. Double-sided α-amylase immunostaining occurring in the electron-dense secretory granules of convoluted granular tubules **(a)**. Double-sided α-amylase amplified immunostaining (large particles) and PNA **(b)** and DBA **(c)** non-amplified staining (small particles). Note the lack of α-amylase reactive sites, at electron-lucent granules of acinar cells, indicated by the absence of large particles on the granule matrix (c). a and b, x 28,300; c, x 26,400

better resist under the electron beam, to avoid the contamination of reagents used on the two faces, as previously observed for control and sialidase-digested specimens (Menghi et al., 1997). However, the following devices were always observed: the silver enhancement was performed after the first binding and this side of the section was coated by a carbon film before the second binding on the opposite side. Visual examination of the binding indicated that the tissues were not over- or under-labeled after silver enhancement.

Some authors preferred to immunolabel one side of the section with one antibody and a probe, then to immunolabel the reverse side with the second antibody and a second sized gold-complex (Bendayan and Stephens, 1984; Beesly, 1989); in addition to their methods, the silver enhancement technique could represent a valid tool to differentiate gold particles of the same size without production of interference on the sensitiveness of the cytochemical marker.

As far as α-amylase distribution is concerned, it emerged that this secretion enzyme is chiefly elaborated by the parotid and submandibular glands. The contribution of the sublingual gland seems to be modest although previous researches have indicated the absence of amylase in the sublingual gland by a substrate film method (Smith et al., 1971). The visualization in situ of the enzyme revealed that in the parotid gland the α-amylase is produced by acini, in the submandibular gland it is synthesized by convoluted granular tubule cells, whereas in the sublingual gland its presence is restricted to demilune secretory granules. A subjective evaluation of the binding intensity did not reveal a differential expression of the enzyme in relation to the known dimorphism of the submandibular gland convoluted granular tubules in the mouse (Lacassagne, 1940; Caramia, 1966). The heterogeneity in amylase and sugar content in different secretory granules here observed could be explained according to Tokunaga and colleagues (1988) who maintain that heterogeneity of glycosylation during secretion can occur.

The combination of the α-amylase immunostaining with the lectin binding on the same section also provided information about the chemical nature of the enzyme. In particular, the lack of α-amylase labeling at electron-lucent granules of the mouse submandibular and sublingual glands revealed that the enzyme, also as glycosylated form, did not contain sialic acid. Indeed, previous (Menghi et al., 1998a,b) and present ultracytochemical findings indicated the presence of sialoglycoconjugates only within the acinar cell electron-lucent granules in both glands. Conversely, in the parotid gland the peculiar location of α-amylase in the electron-dense zones of target granules, where the terminal disaccharide sialic acid-galactose was demonstrated, seems to suggest the occurrence of an isoenzymatic form containing sialic acid with ß-galactose as acceptor sugar. It has been demonstrated that in the human parotid α-amylase, the isoenzyme did not contain sialic acid (Keller et al., 1971). It has also been found that tumor isoamylases are more acidic than salivary-type amylase (Zakowski et al., 1984) and neuraminidase treatment has been variably reported to shift the electrophoretic mobility suggesting that additional sialic acid residues are present in tumor isoamylases (Nakayama et al., 1976; Sudo and Kanno, 1976).

By comparing the rodent salivary glands, it emerged that the mouse parotid gland exhibits rather different amylase distribution on acinar cell secretory granules with respect to the corresponding rat salivary gland (Tanaka et al., 1981; Vugman and Hand, 1995). In addition, differently from rodent, in the human submandibular gland acinar cells, amylase was observed in regions of low and medium electron-density, but not in the dense cores (Takano et al., 1991).

Regarding the combined location of sugars and α-amylase, we were unable to establish colocalization of lectins and enzyme molecule. Indeed, double-sided labeling with only α-amylase on both faces demonstrated that the binding sites of the same molecule are not codistributed on the two faces of the secretory granules in the same section. A similar situation was also observed for the same sugar distribution on the opposite faces of the grid. Although some sugars showed partial overlapping of their reactive sites with those of the enzyme, we cannot establish if this situation is due to binding of reactive sites belonging to different regions of the same molecule, i.e. α-amylase. On a statistical basis, it is possible that the amplification technique on one side

Fig. 6. Sublingual gland. α-amylase immunostaining was only observed on demilunar dark secretory granules **(a)**. Double-sided staining with α-amylase amplified immunogold signal (large particles) on a face and lectins LTA **(b)**, WGA **(c)**, Con A **(d)**, DBA **(e)**, PNA **(f)** non-amplified binding signal (small particles) on the other face illustrates the simultaneous occurrence of sugars and enzyme only on demilunar dark granules. A: Acinar cells. a-d and f, x 26,400; e, x 39,600

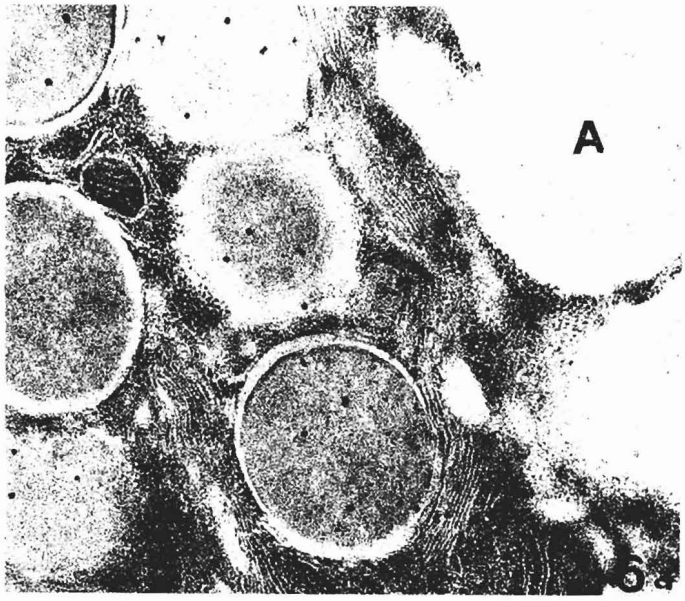

6a

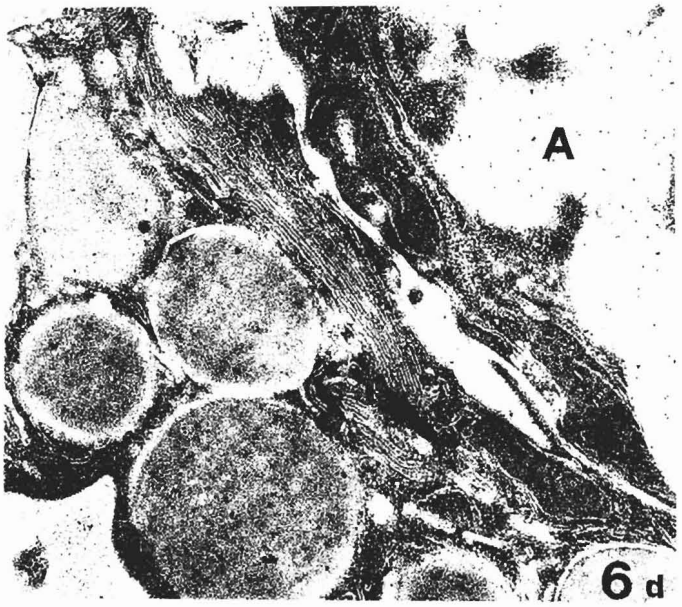

6d

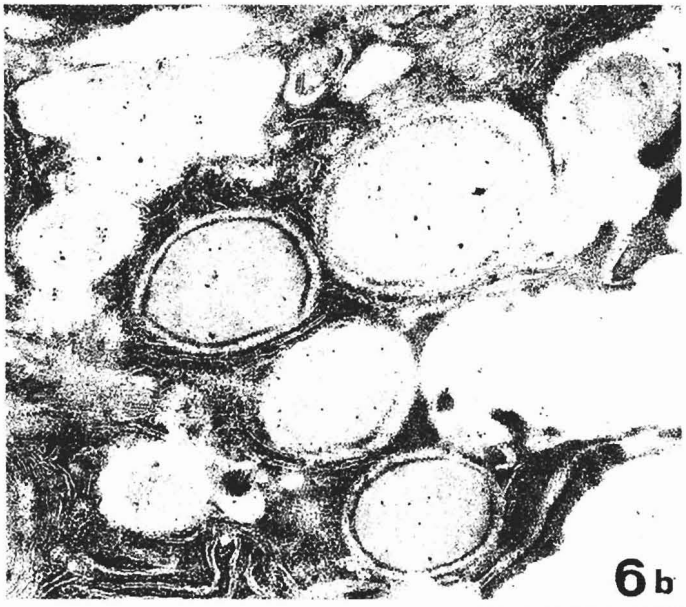

6b

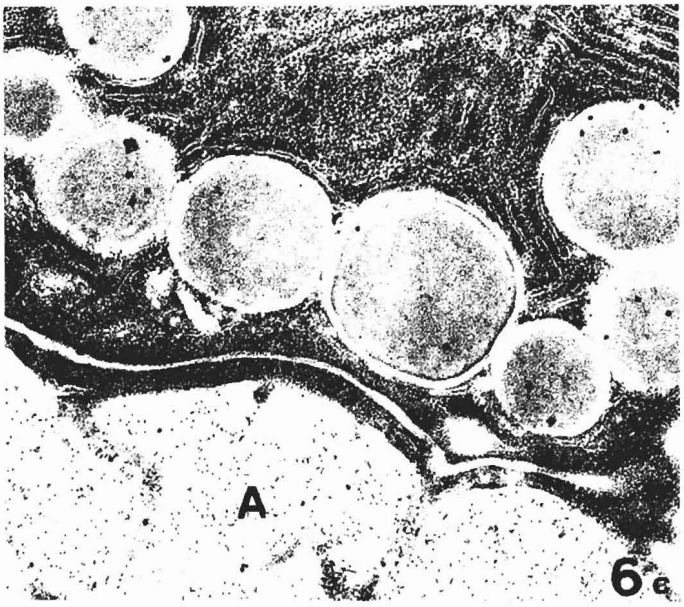

6e

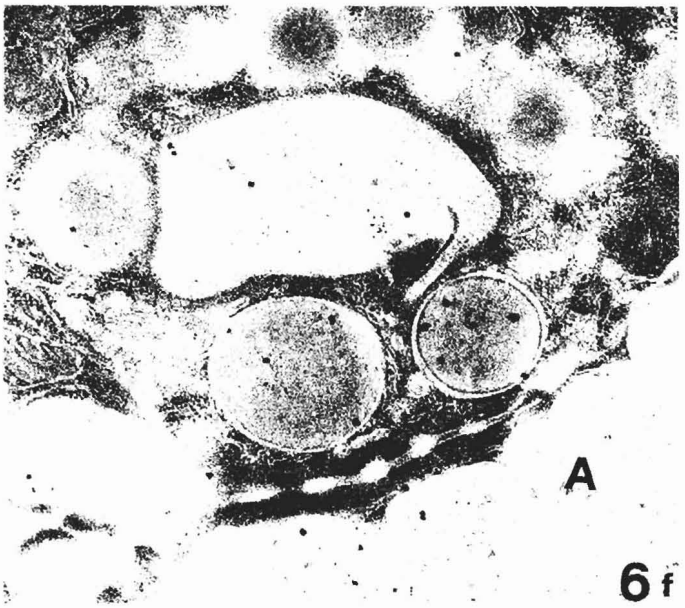

6f

of the section can mask the non amplified gold particles located at the same position on the reverse side.

Acknowledgements. The authors are grateful to Miss. S. Cammertoni and Mr. S. Riccioni for excellent technical assistance. Special thanks are due to Dr. G. Cantalupo (CIGA Center) for carbon coating and Dr. M. Fidani for assisting with electron micrographs. Research was supported by grants from the Italian MURST, CNR and University of Camerino.

References

Beesly J.E. (1989). Colloidal gold: a new perspective for cytochemical marking. Royal Microscopical Society. Microscopy Handbooks. Oxford Science Publications.

Bendayan M. (1995). Colloidal gold post-embedding immunocytochemistry. Progr. Histochem. Cytochem. 29, 1-163.

Bendayan M. and Stephens H. (1984). Double labelling cytochemistry applying the protein α-gold technique. In: Immunolabelling for electron microscopy. Polak J.M. and I.M. Varndell (eds). Elsevier Science Publishers, BV. Amsterdam. pp 143-154.

Buisson G., Duee E., Haser R. and Payan F. (1987). Three dimensional structure of porcine pancreatic alpha α-amylase at 2.9 Å resolution. Role of calcium in structure and activity. EMBO J. 6, 3909-3916.

Caramia F. (1966). Ultrastructure of mouse submaxillary gland. I. Sexual differences. J. Ultrastruct. Res. 16, 505-523.

Hagenbuche O., Bovey R. and Young R.A. (1980). Tissue-specific expression of mouse α-amylase genes: nucleotide sequence of isoenzyme mRNAs from pancreas and salivary gland. Cell 21, 179-187.

Keller P.J., Kauffman D.L., Allan B.J. and Williams B.L. (1971). Further studies on the structural differences between the isoenzymes of human parotid α-amylase. Biochemistry 10, 4867-4874.

Lacassagnae A. (1940). Dimorphisme sexuel de la glande sous maxillaire chez la souris. C. R. Soc. Biol. 133, 180-181.

MacGregor E.A. (1988). α-amylase structure and activity. J. Protein Chem. 7, 399-415.

Mackay R.M., Baird S., Dove M.J., Erratt J.A., Gines M., Moranelli F., Nasim A., Willick G.E., Yaguchi M. and Seligy V.L. (1985). Glucanase gene diversity in prokaryotic and eukaryotic organisms. Biosystems 18, 279-292.

Matsuura Y., Kusunoki M., Harada W. and Kakudo M. (1984). Structure and possible catalytic residues of alpha-amylase. J. Biochem. 95, 697-702.

Meisler M.H. and Gumicio D.L. (1986). Salivary amylase: evolution and tissue specific expression. In: Molecular and cellular basis of digestion. Desnuelle P., Sjostrom H. and Noren O. (eds). Elsevier Science Publishers B.V. Amsterdam.

Menghi G., Bondi A.M., Marchetti L., Gabrielli M.G. and Materazzi G. (1996a). Glycocytochemistry of the mouse parotid gland. Investigation by lectin-gold technique on Bioacryl and Lowicryl K4M embedded specimens. Eur. J. Histochem. 40, 219-234.

Menghi G., Marchetti L., Bondi A.M. and Materazzi G. (1996b). Sialylation patterns of the mouse parotid secretory granules. Combined deacetylation, enzymatic degradation, and lectin-gold binding. Eur. J. Morphol. 34, 181-185.

Menghi G., Marchetti L., Ribichini C., Bondi A.M. and Materazzi G. (1997). Silver enhancement of colloidal gold probes for double lectin labeling at electron microscope level. Eur. J. Histochem. 41/suppl, 46.

Menghi G., Bondi A.M., Marchetti L., Ballarini P. and Materazzi G. (1998a). Confocal and electron microscopy to characterize sialoglycoconjugates in the mouse sublingual gland acinar cells. Eur. J. Morphol. 36, 222-229.

Menghi G., Bondi A.M., Marchetti L., Gabrielli M.G. and Materazzi G. (1998b). Sialoglycoconjugate dimorphism of the mouse submandibular gland acinar cells. Ultrastructural evidence by lectin-protein A-gold probes and sialidase digestion. Histol. Histopathol. 13, 137-146.

Nakajima R., Imanaka T. and Aiba S. (1986). Comparison of aminoacids sequences of eleven different alpha-amylases. Appl. Microbiol. Biotechnol. 23, 355-360.

Nakayama T., Hayashi Y. and Kitamura M. (1976). Amylase isoenzyme found in lung and ovarian cancers. In: Onco-developmental gene expression. Fishman W.H. and Sell S. (eds). Academic Press. New York. pp 455-462.

Smith R.J., Frommer J. and Shiff R. (1971). Localization and onset of amylase activity in mouse salivary glands determined by a substrate film method. J. Histochem. Cytochem. 19, 310-319.

Sudo K. and Kanno T. (1976). Properties of the amylase produced in carcinoma of the lung. Clin. Chim. Acta 73, 1-12.

Takano K., Bogert M., Malamud D., Rally E. and Hand A.R. (1991). Differential distribution of salivary agglutinin and amylase in the Golgi apparatus and secretory granules of human salivary gland acinar cells. Anat. Rec. 230, 307-318.

TanakaT., Gresik W. and Barka T. (1981). Immunocytochemical localization of amylase in the parotid gland of developing and adult rats. J. Histochem. Cytochem. 29, 1189-1195.

Tokunaga M., Kawamura A., Omori A. and Hishinuma F. (1991). Purification and determination of the NH2-terminal aminoacid sequence of mouse amylase secreted from *Saccharomyces cerevisiae*: correct processing of the secretion signal from pGKL killer 28kDa precursor protein. Biochim. Biophys. Acta 1080, 135-137.

Tokunaga M., Kawamura A., Omori A. and Hishinuma F. (1992). Structure of yeast pGKL 128kDa killer-toxin secretion signal sequence. Processing of the 128-kDa killer-toxin-secretion signal—amylase fusion protein. Eur. J. Biochem. 203, 415-423.

Tokunaga M., Wada N. and Hishinuma F. (1987). A novel yeast secretion vector utilizing secretion signal of killer toxin encoded on the yeast linear DNA plasmid PGKL 1. Biochem. Biophys. Res. Commun. 144, 613-619.

Tokunaga M., Wada N. and Hishinuma F. (1988). A novel yeast secretion signal isolated from 28K killer precursor protein encoded on the linear DNA plasmid pGKL1. Nucleic Acid Res. 16, 7499-7511.

Tollefsen S.E. and Rosenblum J.L. (1988). Role of terminal fucose residues in clearance of human glycosylated α-amylase. Am. J. Physiol. 255, G374-G381.

Vugman I. and Hand A.R. (1995). Quantitative immunocytochemical study of secretory protein expression in parotid glands of rats chronically treated with isoproterenol. Microsc. Res. Tech. 31, 106-117.

Zakowski J.J., Gregory M.R. and Bruns D.E. (1984). Amylase from human serous ovarian tumors: purification and characterization. Clin. Chem. 30, 62-68.

Accepted October 29, 1998